DEUTSCHES ELEKTRONEN – SYNCHROTRON

DESY 92-137
October 1992

Formulae and Figures for Basic Two-Body QCD Processes in *ep* Interaction

T. Tymieniecka
NIKHEF, Amsterdam, The Netherlands
and
Institute of Experimental Physics, Warsaw University
A. F. Zarnecki
Institute of Experimental Physics, Warsaw University

ISSN 0418-9833

NOTKESTRASSE 85 · D-2000 HAMBURG 52

DESY 92-137
October 1992

ISSN 0418-9833

Formulae and Figures for Basic Two-Body QCD Processes in *ep* Interaction

Teresa Tymieniecka
NIKHEF, Amsterdam and Institute of Experimental Physics, Warsaw University

Aleksander Filip Żarnecki
Institute of Experimental Physics, Warsaw University

Abstract

A compilation of some useful formulae is given for basic $2 \to 2$ processes involving quarks, gluons and photons. The formulae are illustrated by evaluation of some partonic cross sections, parton luminosities and ep cross sections at HERA and LEP⊗LHC energies.

I. Introduction

The QCD improved parton model provides the framework for studies of high energy hadronic processes at current and future accelerators. In this approach hard hadronic interactions occur through hard two-body elementary subprocesses involving quarks, gluons and gauge bosons.

According to the Standard Model the interaction of electron and proton is mediated in lowest order by exchange of bosons: γ, W, Z. At the energy applicable to *ep* experiments at HERA and at the planned LEP⊗LHC colliders a large cross section is expected for processes with the photon virtuality $Q^2 \approx 0$. This makes the photon an essential participant of two-body subprocesses of interest. It may happen however that the photon does not interact directly with the constituents of the proton. Instead it turns into a vector meson state or simply fragments into a quark-antiquark pair leading then to a partonic cascade. In this case the interaction of the photon with the proton proceeds via the interaction of their partonic constituents. The probability to find a parton in

a photon can be described by a photon structure function analogous to the well known nucleon case.

In the considered approach the leading order cross section for *ep* interactions can be given schematically by convolution of individual probabilities:

$$\sigma^{ep\to ecdX} = \sum_{ab} P_{\gamma/e} \otimes P_{a/\gamma} \otimes P_{b/p} \otimes \hat{\sigma}^{ab\to cd} = \sum_{ab} \mathcal{L}_{ab} \otimes \hat{\sigma}^{ab\to cd}$$

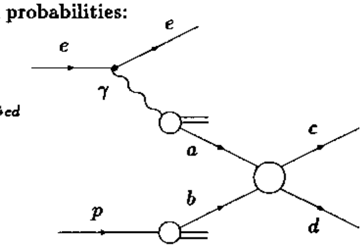

where the sign ⊗ indicates a convolution. One can see that there are two basic ingredients which determine the cross section at the hadron level. The first is a product of probabilities $P_{i/j}$ of finding the relevant constituents i in interacting particles j, the so-called *parton luminosity* $\mathcal{L}_{ab}$. The second is the corresponding *partonic* cross section $\hat{\sigma}$ which describes the interaction of constituents. Each ingredient is the subject of a separate chapter in this note.

Our interest is limited to the elementary $2\to2$ partonic cross sections with photons, quarks and gluons as massless participants. In chapter II we present a compilation of the cross section formulae for the basic, lowest order QCD subprocesses (the Born approximation). They have been collected in [1]. Only formulae for unpolarized cross sections are given. The formulae are illustrated by the corresponding Feynman diagrams. In addition some numerical evaluations are shown to expose the relative contributions of various partonic processes.

The parton luminosity is a product of the parton distributions in the photon and in the proton weighted by a probability of finding the photon in the electron. For studies with the 'untagged' final state electron this probability is described by the Weizsäcker-Williams approximation to a high degree of accuracy[2, 3]. There are many reviews on parton distributions in the nucleon where the main features of the nucleon structure are discussed (e.g. [4, 5]). In contrast information on the photon structure is still limited and contains some theoretical and experimental uncertainty. The present status of knowledge on parton distributions in the photon is reviewed, for example, in [6]. In this paper the parton distributions and resulting from them the parton luminosities are calculated in the leading logarithm approximation. As the parton distributions are deduced from experiment, the luminosities are known only with the present experimental accuracy. Their evaluation is given in chapter III for HERA and LEP⊗LHC energies.

The QCD improved parton model allows the prediction of *ep* cross sections. In chapter IV the *ep* cross sections are evaluated as a function of the invariant masses of the final state partons *cd*. Our goal is to provide an estimate of the order of magnitude of cross sections for selected reactions.

II. Partonic cross section

Two-body elementary parton processes can be described in the Mandelstam variables $s,\ t,\ u$ which are defined as follows:

$$s = (p_a+p_b)^2 = (p_c+p_d)^2$$
$$t = (p_c-p_a)^2 = (p_d-p_b)^2$$
$$u = (p_a-p_d)^2 = (p_b-p_c)^2$$

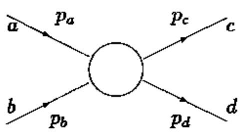

where p_i denotes the four momentum for particle i. In this paper it is assumed that all quarks are massless, therefore, $s+t+u=0$. Traditionally, quantities for subprocesses including the Mandelstam variables are marked by a 'hat' sign, e.g. $\hat{s}$. Here the hats are omitted for transparency.

The basic, lowest order QCD subprocesses are grouped. Thus one subsection contains processes involving only partons: quarks and/or gluons. The subprocesses which apart from partons involve one or two photons are listed in the next two subsections.

II.1. Formulae and diagrams

The formulae for the elementary partonic processes are presented in the following form:

$$\frac{d\hat{\sigma}^{ab\to cd}}{dt} = \frac{\pi}{s^2}\,\hat{G}\,\mathcal{A}(ab\to cd).$$

The term $\mathcal{A}(ab\to cd)$ denotes the squared matrix element, summed over final spins and colours and averaged over the initial ones, however, without coupling constants. The quantity $\hat{G}$ contains the coupling constants for the considered group of subprocesses.

For subprocesses related by crossing symmetry the formulae are displayed only if particles are interchanged between the initial and final state, e.g. $ab\to cd$ and $ac\to bd$. For the others e.g. $ab\to dc$ the proper expressions can be obtained from ones listed below by an appropriate interchange of the Mandelstam variables s,t,u.

II.1.1 The α_s^2 subprocesses (q and g only)

For processes with quarks and gluons only the two-body QCD cross section can be presented in the form [7, 8]:

$$\frac{d\hat{\sigma}^{ab\to cd}}{dt} = \frac{\pi}{s^2}\,\alpha_s^2\,\mathcal{A}(ab\to cd)$$

where the term $\hat{G}$ containing the strong coupling constant α_s is given explicitly $\hat{G}=\alpha_s^2$. The colour factors calculated according to SU(3) of colour, i.e. C_F=4/3 and N_C=3, are included in $\mathcal{A}(ab\to cd)$.

There are eight different 2→2 subprocesses involving only quarks and/or gluons. They are as follows:

1. For $q_iq_j\to q_iq_j$, $i\neq j$, where i and j correspond to the flavour of the quarks

$$\mathcal{A}(q_iq_j\to q_iq_j) = \frac{4}{9}\frac{s^2+u^2}{t^2}.$$

It is the same for $q_i\bar{q}_j\to q_i\bar{q}_j$ and $\bar{q}_i\bar{q}_j\to \bar{q}_i\bar{q}_j$ $(i\neq j)$. The corresponding Feynman diagram is shown in Fig.1.

2. For $q_iq_i\to q_iq_i$ (or $\bar{q}_i\bar{q}_i\to\bar{q}_i\bar{q}_i$), see Fig.2 for corresponding diagrams

$$\mathcal{A}(q_iq_i\to q_iq_i) = \frac{4}{9}\left(\frac{s^2+u^2}{t^2}+\frac{s^2+t^2}{u^2}\right) - \frac{8}{27}\frac{s^2}{tu}.$$

3. For $\bar{q}_iq_i\to\bar{q}_jq_j$, $i\neq j$ (see Fig.3)

$$\mathcal{A}(\bar{q}_iq_i\to\bar{q}_jq_j) = \frac{4}{9}\frac{t^2+u^2}{s^2}.$$

4. For $\bar{q}_iq_i\to\bar{q}_iq_i$ (see Fig.4)

$$\mathcal{A}(\bar{q}_iq_i\to\bar{q}_iq_i) = \frac{4}{9}\left(\frac{s^2+u^2}{t^2}+\frac{u^2+t^2}{s^2}\right) - \frac{8}{27}\frac{u^2}{st}.$$

5. For $\bar{q}_iq_i\to gg$ (see Fig.5)

$$\mathcal{A}(\bar{q}_iq_i\to gg) = \frac{32}{27}\frac{u^2+t^2}{ut} - \frac{8}{3}\frac{u^2+t^2}{s^2}.$$

6. For $gg\to q_i\bar{q}_i$ (see Fig.6)

$$\mathcal{A}(gg\to q_i\bar{q}_i) = \frac{1}{6}\frac{u^2+t^2}{ut} - \frac{3}{8}\frac{u^2+t^2}{s^2}.$$

7. For $gq_i\to gq_i$ (or $g\bar{q}_i\to g\bar{q}_i$, see Fig.7)

$$\mathcal{A}(gq_i\to gq_i) = -\frac{4}{9}\frac{u^2+s^2}{us} + \frac{u^2+s^2}{t^2}.$$

8. For $gg\to gg$ (see Fig.8)

$$\mathcal{A}(gg\to gg) = \frac{9}{2}\left(3 - \frac{ut}{s^2} - \frac{us}{t^2} - \frac{st}{u^2}\right).$$

II.1.2 The $\alpha_s\alpha$ subprocesses (one γ in the final or initial state)

The lowest order, two-body cross section for these subprocesses can be presented, as previously, in the form:

$$\frac{d\hat{\sigma}^{ab\to cd}}{dt} = \frac{\pi}{s^2}\,\alpha_s\alpha\, {e_i}^2\, \mathcal{A}(ab \to cd)$$

where α is the electromagnetic coupling constant and e_i stands for the charge of the involved quark. Other symbols are defined as in the previous section.

There are four 2→2 subprocesses of order $\alpha_s\alpha$. The formulae for $\mathcal{A}(ab \to cd)$ have the following form [9]:

1. For $\bar{q}_i q_i \to \gamma g$ (see Fig.9)

$$\mathcal{A}(\bar{q}_i q_i \to \gamma g) = \frac{8}{9}\frac{u^2+t^2}{ut}.$$

2. For $\gamma g \to q_i\bar{q}_i$ (see Fig.10)

$$\mathcal{A}(\gamma g \to q_i\bar{q}_i) = \frac{u^2+t^2}{ut}.$$

3. For $g q_i \to \gamma q_i$ (or $g\bar{q}_i \to \gamma\bar{q}_i$, see Fig.11)

$$\mathcal{A}(g q_i \to \gamma q_i) = -\frac{1}{3}\frac{u^2+s^2}{us}.$$

4. For $\gamma q_i \to g q_i$ (or $\gamma\bar{q}_i \to g\bar{q}_i$, see Fig.12)

$$\mathcal{A}(\gamma q_i \to g q_i) = -\frac{8}{3}\frac{u^2+s^2}{us}.$$

II.1.3 The α^2 subprocesses (with two γ)

For subprocesses with two photons in the final and/or initial state we have:

$$\frac{d\hat{\sigma}^{ab\to cd}}{dt} = \frac{\pi}{s^2}\,\alpha^2\, {e_i}^4\, \mathcal{A}(ab \to cd).$$

As before α is the electromagnetic coupling constant and e_i stands for the charge of the involved quark.

1. For $\bar{q}_i q_i \to \gamma\gamma$ (see Fig.13)

$$\mathcal{A}(\bar{q}_i q_i \to \gamma\gamma) = \frac{2}{3}\frac{u^2+t^2}{ut}.$$

2. For $\gamma\gamma \to q_i\bar{q}_i$ (see Fig.14)

$$\mathcal{A}(\gamma\gamma \to q_i\bar{q}_i) = 6\,\frac{u^2+t^2}{ut}.$$

3. For $\gamma q_i \to \gamma q_i$ (or $\gamma\bar{q}_i \to \gamma\bar{q}_i$, see Fig.15)

$$\mathcal{A}(\gamma q_i \to \gamma q_i) = -2\,\frac{u^2+s^2}{us}.$$

II.2. Numerical evaluation of partonic cross sections

In order to expose the relative contributions of the listed two-body QCD processes some partonic cross sections are evaluated. It is convenient to present them as angular distributions in the partonic ab centre-of-mass frame:

$$\frac{d\hat{\sigma}^{ab\to cd}}{dcos(\theta)} = \frac{s}{2}\frac{d\hat{\sigma}}{dt} = \frac{\pi}{2\,s}\,\hat{G}\,\mathcal{A}(ab\to cd)$$

where the scattering angle θ between partons a and c is given by $t=-s/2\cdot(1-cos(\theta))$. The quantities $\hat{G}$ and $\mathcal{A}(ab\to cd)$ are defined and displayed in section II.1.

Note that for massless particles the ratios of Mandelstam variables t/s, t/u and u/s are functions of $cos(\theta)$ alone. Therefore, the term $\mathcal{A}(ab\to cd)$ is a function of $cos(\theta)$ only and, besides the running of coupling constants hidden in the $\hat{G}$ term, the sole energy dependence of the differential partonic cross section comes from the explicitly given squared energy s. In order to obtain the partonic cross section at an energy of interest s' one can scale the cross section evaluated at the energy s according to the ratio s/s'. In more exact calculations the $\hat{G}$ dependence on energy should be included.

In this paper the energy of the incoming partons ab, or the outgoing partons cd, is expressed by their invariant mass $M=\sqrt{s}$.

For illustration, the following values are adopted: the invariant mass M is taken to be 50 GeV; the strong coupling constant α_s=0.15; the electromagnetic coupling constant α=1/137. The calculations are done for u-quarks, i.e. $q(\bar{q})$ denotes the $u(\bar{u})$-quark while q' denotes any of the d,s,c,b-quarks.

The results of the numerical evaluations for the $ab\to cd$ subprocesses are presented in Figs 16-20 as follows. Fig.16 shows the partonic cross section for subprocesses involving quarks or antiquarks in the initial state. Each annihilation process $\bar{q}q$ is a representative process for the different group of subprocesses. Notice the differences in cross sections between them coming from the coupling constants. The next three drawings show the partonic cross sections for subprocesses with photons in the initial or final state. Fig.17 contains those with one photon (listed in section II.1.2). The subprocesses with two photons as listed in section II.1.3 are given in Fig.18. Fig.19 displays cross sections for one photon in the final state. The last drawing Fig.20 shows the partonic cross sections for subprocesses where both, gluons and quarks, are involved.

These numerical evaluations exhibit the kinematical properties of the matrix elements expressed in this paper by the term $\mathcal{A}(ab\to cd)$. In particular, note the discontinuities around the scattering angle θ=0 and $\theta=\pi$. It is due to the t-pole and the u-pole in the term $\mathcal{A}(ab\to cd)$. Notice also that cross sections for some subprocesses differ by a constant factor only, i.e. the coupling constants and the colour factors; for example, $\gamma q\to\gamma q$ and $\gamma q\to gq$.

III. Parton luminosity

As an illustration of the physics potential in ep interaction at the HERA energy $\sqrt{S}$=314 GeV and at the LEP⊗LHC energy $\sqrt{S}$=1300 GeV the differential parton luminosity is evaluated for a few selected processes. This quantity represents the probability of parton-parton (parton-photon) interactions in ep collisions. As such, it exhibits the relative contribution of direct photon processes (the left diagram) to those where the hadronic structure of the photon is involved (the right diagram). The luminosity has been investigated in studies for hadron-hadron colliders [10] as well as for HERA [11].

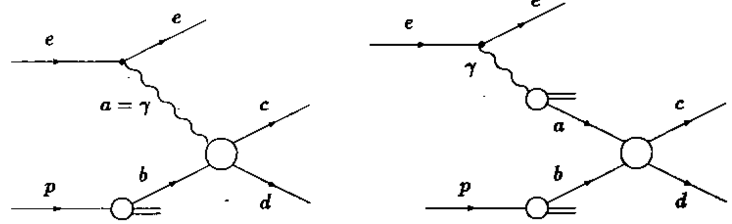

Since the involved partons ab carry only a fraction of the incident energy a convenient way to quantify luminosity is to show it as a function of their invariant mass M^2. Thus, the luminosity is given as:

$$\frac{d\mathcal{L}^{ep\to ab}}{dM^2} = \int_0^1 dx_\gamma \int_0^1 dx_a \int_0^1 dx_b\, P_{\gamma/e}(x_\gamma)\, P_{a/\gamma}(x_a,M^2)\, P_{b/p}(x_b,M^2)\, \delta(M^2-x_a x_b x_\gamma S)$$

which leads to:

$$\frac{d\mathcal{L}^{ep\to ab}}{dM} = \frac{2M}{S}\int_\tau^1 \frac{dx_\gamma}{x_\gamma}\, P_{\gamma/e}(x_\gamma) \int_{\frac{\tau}{x_\gamma}}^1 \frac{dx_a}{x_a}\, P_{a/\gamma}(x_a,M^2)\, P_{b/p}(\frac{\tau}{x_\gamma x_a},M^2)$$

where $\tau=M^2/S$ with $\sqrt{S}$ to be the total energy of ep collision in the centre-of-mass system. The function $P_{\gamma/e}(x_\gamma)$ denotes the probability of finding a photon in the electron as provided by the Weizsäcker-Williams approximation:

$$P_{\gamma/e}(x_\gamma) = \frac{\alpha}{2\pi}\frac{1+(1-x_\gamma)^2}{x_\gamma}\ln\frac{E^2}{4m_e^2}$$

where m_e is the electron mass and x_γ is a fraction of the electron's energy carried by the photon. The scale E^2 in the logarithmic term of the Weizsäcker-Williams formula is taken to be $E^2=M^2$. Some discussion of its possible form can be found, for example, in [12]. The functions $P_{a/\gamma}(x_a,M^2)$ and $P_{b/p}(x_b,M^2)$ are the parton density of a in the photon and the parton density of b in the proton with $a=\gamma,g,q,\bar{q}$ and $b=g,q,\bar{q}$. The species a carries a fraction x_a of photon momentum whereas the species b carries the corresponding fraction x_b of proton momentum. Note that the scale M^2 is used in both the structure function for the photon and the proton.

The application of the Weizsäcker-Williams formalism called sometimes the equivalent photon approximation implies that the exchanged photons are effectively real – on shell and collinear with the ep beams – with their virtuality $Q^2 \approx 0$. To get a feeling of discrepancies between this approach and more exact techniques the reader is referred to, for example [13, 14].

In the numerical evaluation of parton densities in the proton we used the Morfin and Tung (MT) parameterization, set 0, [15] as provided by the code[16]. This parameterization is obtained in the leading order QCD approximation with $\Lambda_{QCD} = 0.144$ GeV and for 6 quark flavours with thresholds for c, b and t-production. For the parton density in the photon the Drees and Grassie parameterization, set 1, [17] is taken again as provided by the code[18] except for the direct contribution $a = \gamma$ where $P_{a/\gamma}(x_a, M^2)=\delta(x_a - 1)$ is taken. The DG parameterization of the photon structure function is given for the number of quark flavours changing with the M^2 scale from N_f=3 to N_f=5.

The results of calculations for the various initial states ab are presented in Figs 21-24. The quark u is considered mainly; therefore $q(\bar{q})$ denotes the $u(\bar{u})$-quark whereas the symbol q' (or $\bar{q}'$) refers to a sum over the d, s, c, b-quarks. Effects of the b-quark threshold are visible in Fig. 22. Notice that the partonic distribution for antiquarks in the photon is the same as for quarks. It leads to the same luminosity for processes with $a = q$ and $a = \bar{q}$, for example, $\bar{q}q$ and qq. For clarity the $\bar{q}$ subprocesses are not shown in the figures.

IV. ep cross section

The aim of this section is to present individual contributions of the subprocesses $ab \rightarrow cd$ to ep cross section at the HERA energy $\sqrt{S}$=314 GeV and at the LEP⊗LHC energy $\sqrt{S}$=1300 GeV. The calculations are done in the leading order of QCD. It is worth noting that the next-to-leading-order corrections might not be negligible; to get a feeling of their size the reader is referred to e.g. [19, 20].

The differential cross section is shown as a function of invariant mass M of the involved partons ab (or cd), however, with a cut on transverse momentum of the outgoing partons cd. This cut avoids divergences around the parton emission angle θ=0 and $\theta=\pi$ with respect to incoming partons. Here θ is again defined in the ab centre-of-mass system (see sect. II.2). The cut value can be chosen such as to remove partons which are not detected due to the finite size of the collider beam pipe.

The cross section for ep interaction is given in leading order as a product of the partonic cross section $d\hat{\sigma}/dcos(\theta)$ and the parton luminosity $d\mathcal{L}/dM$

$$\frac{d\sigma^{ep\rightarrow cdX}}{dM} = \sum_{ab} \frac{d\mathcal{L}^{ep\rightarrow ab}}{dM} \int_{-cos(\theta_0)}^{+cos(\theta_0)} \frac{d\hat{\sigma}^{ab\rightarrow cd}(M, cos(\theta))}{dcos(\theta)} dcos(\theta).$$

They are described in some details in chapters II and III. A cut p_T on the transverse momentum is implemented via $cos(\theta_0) = \sqrt{1 - 4p_T^2/M^2}$. Be aware that any transverse motion of 'intermediating' species γ, a and b is totally neglected. The label X denotes remnants of the disintegrated proton and photon.

The numerical evaluation is done for the value of the transverse momentum cut p_T equal to 2 GeV/c for the HERA energy and to 10 GeV/c for the LEP⊗LHC energies. The running coupling constant:

$$\alpha_s(M^2) = \frac{12\pi}{(33 - 2N_f)\ln\left(M^2/\Lambda_{QCD}^2\right)}$$

is taken for Λ_{QCD}=0.144 GeV as in the MT parameterization. The electromagnetic coupling constant α is fixed at 1/137.

The main calculations are done for u-quarks with results for the HERA energy presented as follows. Fig.25 shows the ep cross section for subprocesses where photons are involved. Fig.26 contains subprocesses with gluons in the final state while Fig.27 shows ep cross sections for production of quarks alone. The ep cross section for $gg \rightarrow gg$ or $qq \rightarrow qq$ is included in Figs 25-27 as reference points in the visual comparison between subprocesses.

To display the contribution of flavours other than the previously considered u-quark we present ep cross sections summed over all the possible flavours for subprocesses with photons in the final state Fig.28.

Similar numerical evaluations are presented in Figs 29-31 for the LEP⊗LHC energies.

V. Summary

In this note some formulae of general application are collected and illustrated by some numerical evaluations. The leading order approach are used for massless quarks.

The displayed formulae contain the basic partonic cross sections for two-body processes involving quarks, gluons and photons. Although this compilation is dedicated to subprocesses in *ep* interactions these formulae are of interest in the study of hadron-hadron, lepton-lepton as well as lepton-hadron interactions.

Parton luminosities in *ep* interactions intermediated by the almost real photon $Q^2 \approx 0$ are discussed for the direct photon interaction and the photon interacting via its hadronic structure.

The collected formulae are used to investigate two-body processes involved in *ep* interaction. Their individual contributions to the total cross section are evaluated at the HERA and LEP⊗LHC energies. The partonic cross sections are given in the form of angular distributions of the outgoing partons in their centre-of-mass frame; the contributions to the *ep* cross section are shown as a function of the total energy carried by the partons in this frame (their invariant mass). A minimum transverse momentum is imposed on the outgoing partons to avoid singularities.

The presented results should provide better understanding of the relative contribution of multijet events and their structure at HERA or LEP⊗LHC. The discussion of the absolute magnitudes of the individual contributions goes beyond the purpose of this note. One can state however that the perturbative part of the HERA physics is overwhelmed by subprocesses involving the hadronic structure of the photon and the *ep* collider at the LEP⊗LHC energy could almost be called a gluon factory. This summary of cross sections can help in the choice of the physical field of interest and therefore, in the design of detectors for the future LEP⊗LHC experiments.

Acknowledgements

We would like to thank M.Krawczyk for her important contribution to this paper. We are indebted to P.M.Kooijman, G.Wolf and J.Zakrzewski for careful and critical reading of the manuscript. We acknowledge the financial support of the Polish Committee for Scientific Research KBN PB 1071/2/91.

References

[1] M.Krawczyk, A.F.Zarnecki, Basic two body QCQ processes in formulae and figures, Institute of Theoretical Physics, Warsaw University, report IFT 08/91, 1991.

[2] H.Kolanoski, Two photon physics at e^+e^- storage rings, Springer Tracts in Modern Physics, vol.105, 1984.

[3] V.M.Budnev,I.F.Ginzburg, G.V.Meledin, V.G.Serbo, Phys.Rep. 15C(1974)181.

[4] Wu-Ki Tung, Nucl.Phys. B315(1989)378.
Wu-Ki Tung et al., ANL-HEP-CP-89-01.

[5] K.Charchula et al., DESY 90-019,1990.

[6] H.Abramowicz et al., DESY 91-057,1991.

[7] J.F.Owens, E.Reya, M.Glück, Phys.Rev. D18(1978)1501.

[8] B.L.Combridge, J.Kripfganz, J.Ranft, Phys.Let. 70B(1977)234.

[9] D.W.Duke, J.F.Owens, Phys.Rev. D26(1982)1600.

[10] R.K.Eichten, I.Hinchliffe, K.Lane, C.Quigg, Rev.Mod.Phys., 56(1984)579.

[11] R.K.Ellis, Z.Kunszt, Nucl.Phys. B303(1988)653.

[12] M.Drees, R.M.Godbole, Phys.Rev. D39(1989)169.

[13] A.Zembrzuski, M.Krawczyk, Physics at HERA, Proceedings of the Workshop, Hamburg, 1991, p.617, ed. W.Buchmüller, G.Ingelman.

[14] G.A.Schuler, Nucl.Phys. B299(1988)21.

[15] J.Morfin, Wu-Ki Tung, Zeit.Phys. C52(1991)13.

[16] K.Charchula, Comp.Phys.Comm. 69(1992)360.

[17] M.Drees, K.Grassie, Zeit.Phys. C28(1985)451.

[18] K.Charchuła, ZEUS-Note 91-073, 1991.

[19] D.Bödeker, Physics at HERA, Proceedings of the Workshop, Hamburg, 1991, p.657, ed. W.Buchmüller, G.Ingelman.

[20] H.Baer, J.Ohnemus, J.F.Owens, Phys.Rev. D40(1989)2844.

Figure captions

Fig.1 Feynman diagram for $q_i q_j \to q_i q_j$, $i \neq j$.

Fig.2 Feynman diagrams for $q_i q_i \to q_i q_i$.

Fig.3 Feynman diagram for $\bar{q}_i q_i \to \bar{q}_j q_j$, $i \neq j$.

Fig.4 Feynman diagrams for $\bar{q}_i q_i \to \bar{q}_i q_i$.

Fig.5 Feynman diagrams for $\bar{q}_i q_i \to gg$.

Fig.6 Feynman diagrams for $gg \to q_i \bar{q}_i$.

Fig.7 Feynman diagrams for $gq_i \to gq_i$.

Fig.8 Feynman diagrams for $gg \to gg$.

Fig.9 Feynman diagrams for $\bar{q}_i q_i \to \gamma g$.

Fig.10 Feynman diagrams for $\gamma g \to q_i \bar{q}_i$.

Fig.11 Feynman diagrams for $gq_i \to \gamma q_i$.

Fig.12 Feynman diagrams for $\gamma q_i \to gq_i$.

Fig.13 Feynman diagrams for $\bar{q}_i q_i \to \gamma\gamma$.

Fig.14 Feynman diagrams for $\gamma\gamma \to q_i \bar{q}_i$.

Fig.15 Feynman diagrams for $\gamma q_i \to \gamma q_i$.

Fig.16 The partonic cross section for subprocesses $ab \to cd$ involving quarks or antiquarks in the initial state as a function of the scattering angle $cos(\theta)$ between partons a and c in the ab centre-of-mass for the invariant mass $M = \sqrt{s} = 50$ GeV. Note that the label $q(\bar{q})$ denotes the $u(\bar{u})$-quark while q' and $\bar{q}'$ refer to a sum over the d, s, c, b-quarks and antiquarks respectively.

Fig.17 The partonic cross section for subprocesses $ab \to cd$ involving a photon in the initial or final state as a function of the scattering angle $cos(\theta)$ between partons a and c in the ab centre-of-mass for the invariant mass $M = \sqrt{s} = 50$ GeV.

Fig.18 The partonic cross section for subprocesses $ab \to cd$ involving two photons in the initial or final state as a function of the scattering angle $cos(\theta)$ between partons a and c in the ab centre-of-mass for the invariant mass $M = \sqrt{s} = 50$ GeV.

Fig.19 The partonic cross section for subprocesses $ab \to cd$ involving one photon in the final state as a function of the scattering angle $cos(\theta)$ between partons a and c in the ab centre-of-mass for the invariant mass $M = \sqrt{s} = 50$ GeV.

Fig.20 The partonic cross section for subprocesses $ab \to cd$ involving gluons and quarks in the final state as a function of the scattering angle $cos(\theta)$ between partons a and c in the ab centre-of-mass for the invariant mass $M = \sqrt{s} = 50$ GeV.

Fig.21 The parton luminosity for subprocesses involving photons (dashed lines), gluons with quarks/antiquarks (dotted lines), gluon-gluon (full line) and quarks only (dashed-dotted lines) for $\sqrt{S}$=314 GeV. M is the invariant mass of the listed partons. Note that the label $q(\bar{q})$ denotes the $u(\bar{u})$-quark. The first label refers to the photon component whereas the second one refers to the parton originating from the proton.

Fig.22 The parton luminosity for subprocesses involving quarks only for $\sqrt{S}$=314 GeV. M is the invariant mass of the listed partons. Note that the label $q(\bar{q})$ denotes the $u(\bar{u})$-quark while q' and $\bar{q}'$ refer to a sum over the d, s, c, b-quarks and antiquarks respectively. The first label refers to the photon component whereas the second one refers to the parton originating from the proton.

Fig.23 The parton luminosity for subprocesses involving photons (dashed lines), gluons with quarks/antiquarks (dotted lines), gluon-gluon (full line) and quarks only (dashed-dotted lines) for $\sqrt{S}$=1.3 TeV. M is the invariant mass of the listed partons. Note that the label $q(\bar{q})$ denotes the $u(\bar{u})$-quark. The first label refers to the photon component whereas the second one refers to the parton originating from the proton.

Fig.24 The parton luminosity for subprocesses involving quarks only for $\sqrt{S}$=1.3 TeV. M is the invariant mass of the listed partons. Note that the label $q(\bar{q})$ denotes the $u(\bar{u})$-quark while q' and $\bar{q}'$ refer to a sum over the d, s, c, b-quarks and antiquarks respectively. The first label refers to the photon component whereas the second one refers to the parton originating from the proton.

Fig.25 The ep cross section for subprocesses involving photons (dotted lines), gluons (full lines) and quarks only (dashed lines) in the final state for $\sqrt{S}$=314 GeV. M is the invariant mass of the outgoing partons. Note that $q(\bar{q})$ denotes the $u(\bar{u})$-quark. The first label refers to the photon component whereas the second one refers to the parton originating from the proton.

Fig.26 The ep cross section for subprocesses involving gluons in the final state and $qq \to qq$ (see text) for $\sqrt{S}$=314 GeV. M is the invariant mass of the outgoing partons. Note that the label $q(\bar{q})$ denotes the $u(\bar{u})$-quark. The first label refers to the photon component whereas the second one refers to the parton originating from the proton.

Fig.27 The ep cross section for subprocesses involving quarks in the final state for $\sqrt{S}$=314 GeV. M is the invariant mass of the outgoing partons. Note that the label $q(\bar{q})$ denotes the $u(\bar{u})$-quark while q' and $\bar{q}'$ refer to a sum over the d, s, c, b-quarks and antiquarks respectively. The first label refers to the photon component whereas the second one refers to the parton originating from the proton.

Fig.28 The ep cross section for subprocesses leading to photons in the final state for $\sqrt{S}$=314 GeV. M is the invariant mass of the outgoing partons. Note that here q refers to a sum over the d, u, s, c, b-quarks and their anti-quarks in the proton; the label $q\bar{q}$ denotes a sum over all pairs $q\bar{q}$ in the photon and the proton; the label gq refers to a sum over all pairs of quarks(antiquarks) and gluons in the photon and the proton.

Fig.29 The ep cross section for subprocesses involving photons (dotted lines), gluons (full lines) and quarks only (dashed lines) in the final state for $\sqrt{S}$=1.3 TeV. M is the invariant mass of the outgoing partons. Note that $q(\bar{q})$ denotes the $u(\bar{u})$-quark respectively. The first label refers to the photon component whereas the second one refers to the parton originating from the proton.

Fig.30 The ep cross section for subprocesses involving gluons in the final state (full lines) and quarks only (dashed and dashed-dotted lines) for $\sqrt{S}$=1.3 TeV. M is the invariant mass of the outgoing partons. Note that the label $q(\bar{q})$ denotes the $u(\bar{u})$-quark while q' and $\bar{q}'$ refer to a sum over the d, s, c, b-quarks and antiquarks respectively. The first label refers to the photon component whereas the second one refers to the parton originating from the proton.

Fig.31 The ep cross section for subprocesses leading to photons in the final state for $\sqrt{S}$=1.3 TeV. M is the invariant mass of the outgoing partons. Note that here q refers to a sum over the d, u, s, c, b-quarks and their anti-quarks in the proton; the label $q\bar{q}$ denotes a sum over all pairs $q\bar{q}$ in the photon and the proton; the label gq refers to a sum over all pairs of quarks(antiquarks) and gluons in the photon and the proton.

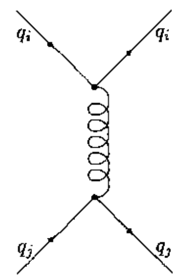

Figure 1: Feynman diagram for $q_iq_j \to q_iq_j$, $i \neq j$

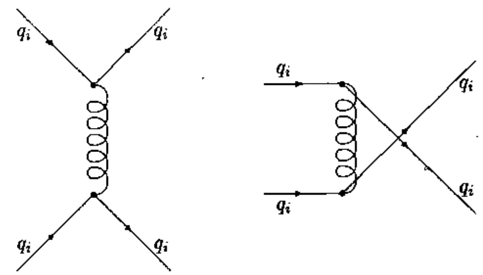

Figure 2: Feynman diagrams for $q_iq_i \to q_iq_i$

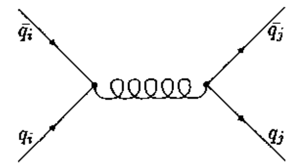

Figure 3: Feynman diagram for $\bar{q}_iq_i \to \bar{q}_jq_j$, $i \neq j$

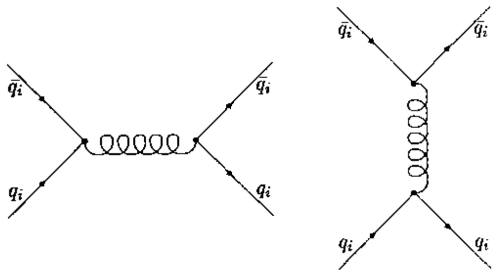

Figure 4: Feynman diagrams for $\bar{q}_i q_i \to \bar{q}_i q_i$

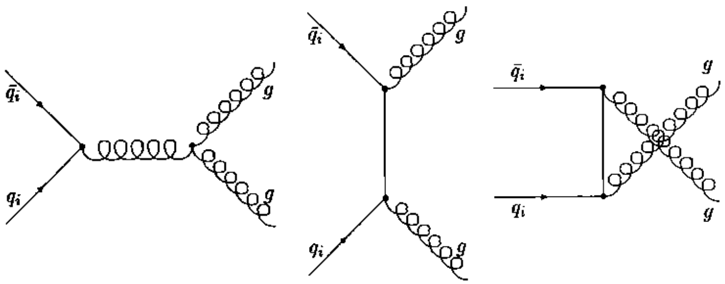

Figure 5: Feynman diagrams for $\bar{q}_i q_i \to gg$

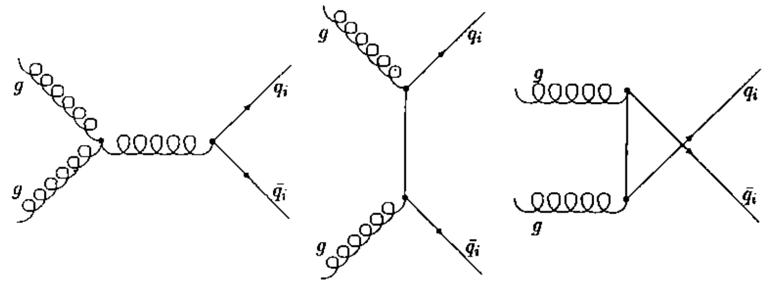

Figure 6: Feynman diagrams for $gg \to q_i \bar{q}_i$

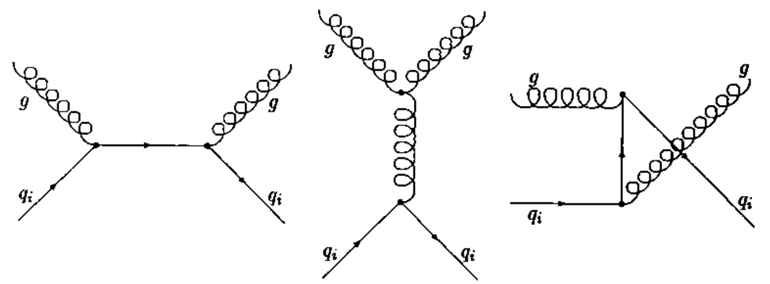

Figure 7: Feynman diagrams for $gq_i \to gq_i$

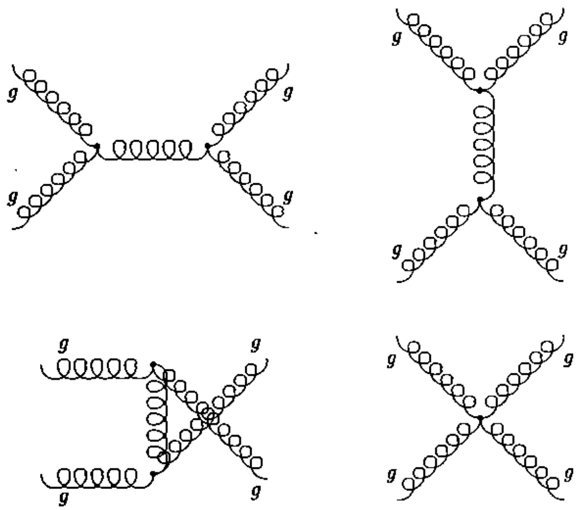

Figure 8: Feynman diagrams for $gg \to gg$

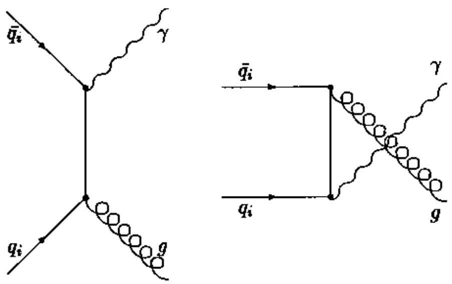

Figure 9: Feynman diagrams for $\bar{q}_i q_i \to \gamma g$

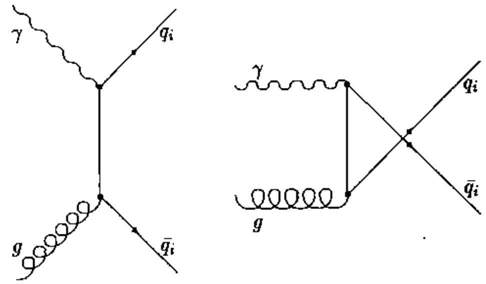

Figure 10: Feynman diagrams for $\gamma g \to q_i \bar{q}_i$

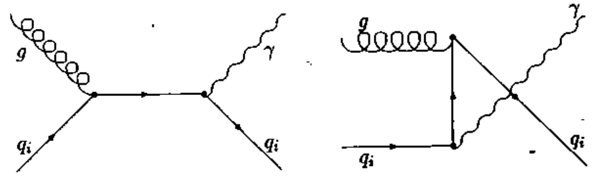

Figure 11: Feynman diagrams for $g q_i \to \gamma q_i$

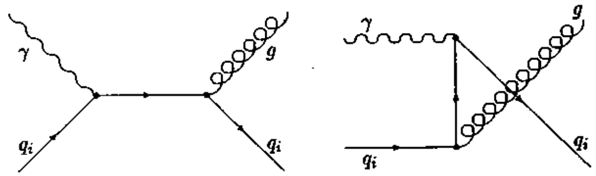

Figure 12: Feynman diagrams for $\gamma q_i \to g q_i$

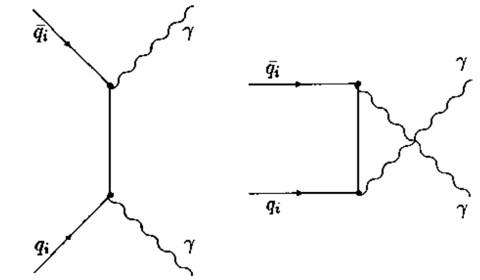

Figure 13: Feynman diagrams for $\bar{q}_i q_i \to \gamma\gamma$

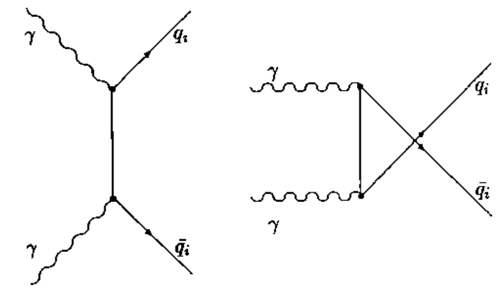

Figure 14: Feynman diagrams for $\gamma\gamma \to q_i \bar{q}_i$

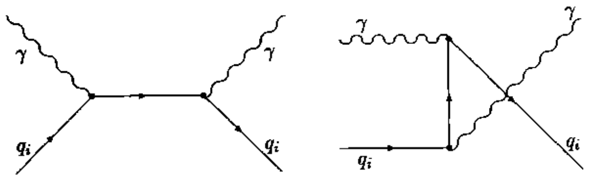

Figure 15: Feynman diagrams for $\gamma q_i \to \gamma q_i$

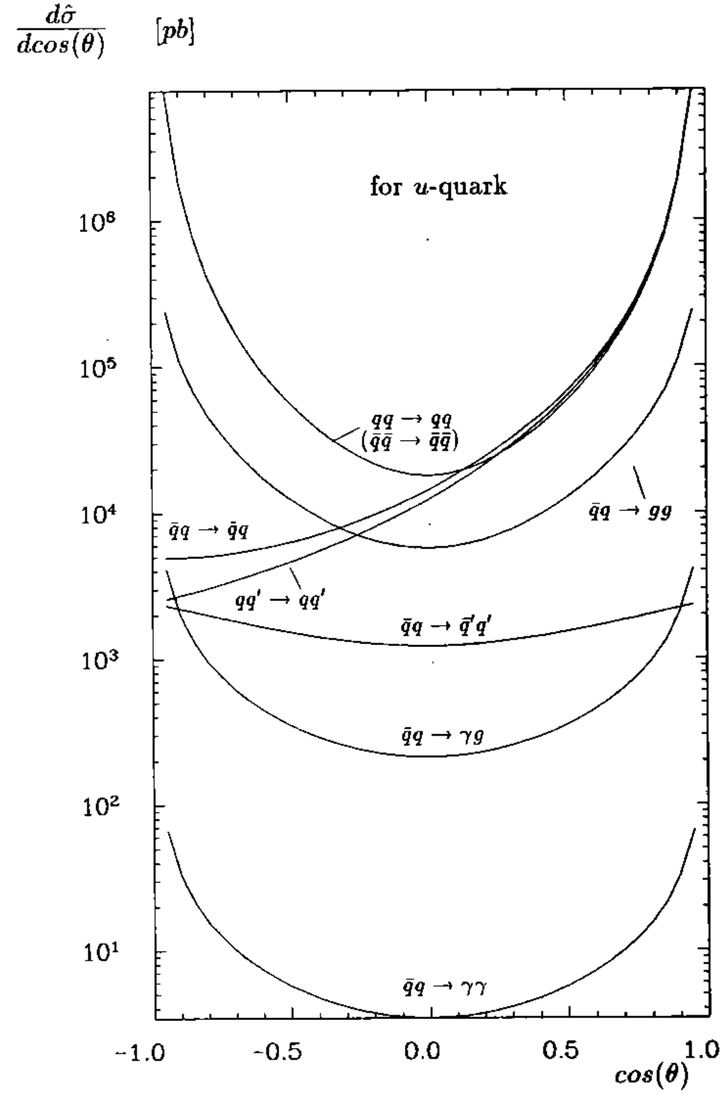

Figure 16: The partonic cross section for subprocesses $ab \to cd$ involving quarks or antiquarks in the initial state as a function of the scattering angle $cos(\theta)$ between partons a and c in the ab centre-of-mass for the invariant mass $M = \sqrt{\hat{s}} = 50$ GeV. Note that the label $q(\bar{q})$ denotes the $u(\bar{u})$-quark while q' and $\bar{q}'$ refer to a sum over the d, s, c, b-quarks and antiquarks respectively.

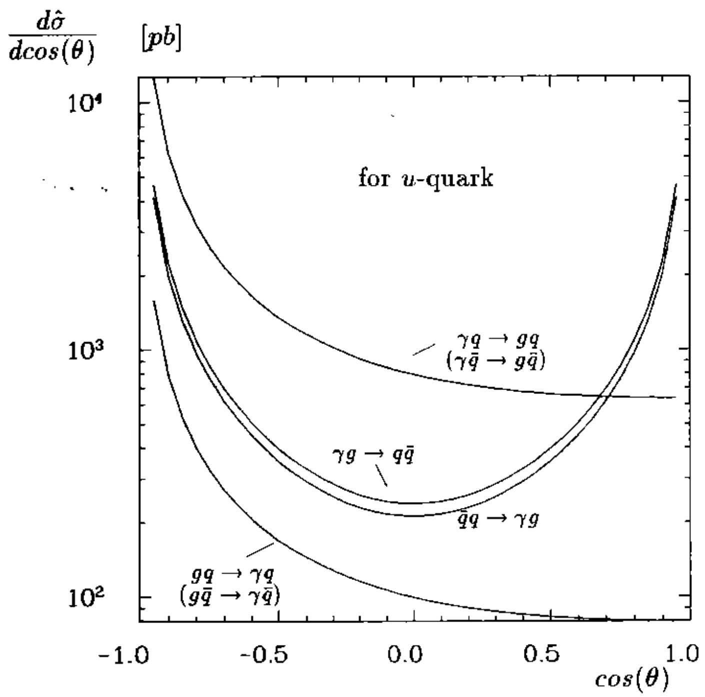

Figure 17: The partonic cross section for subprocesses $ab \to cd$ involving a photon in the initial or final state as a function of the scattering angle $cos(\theta)$ between partons a and c in the ab centre-of-mass for the invariant mass $M = \sqrt{s} = 50$ GeV.

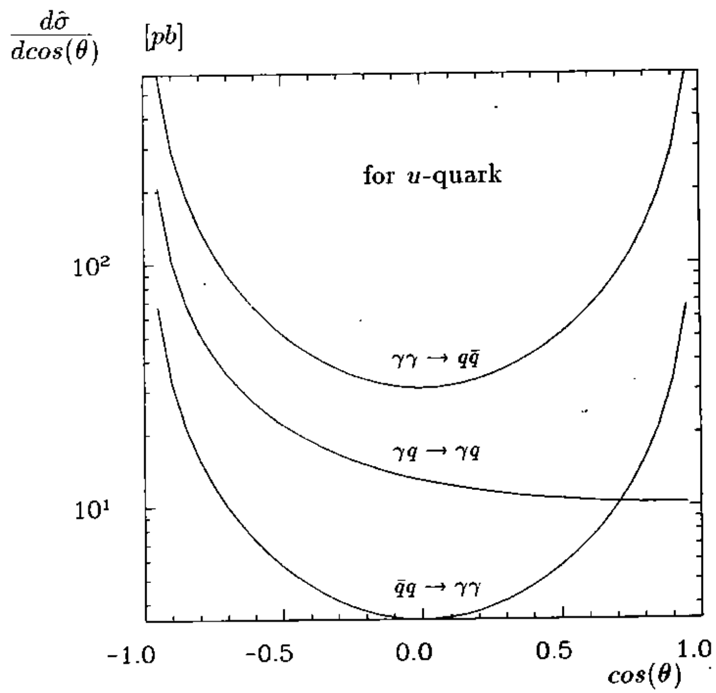

Figure 18: The partonic cross section for subprocesses $ab \to cd$ involving two photons in the initial or final state as a function of the scattering angle $cos(\theta)$ between partons a and c in the ab centre-of-mass for the invariant mass $M = \sqrt{s} = 50$ GeV.

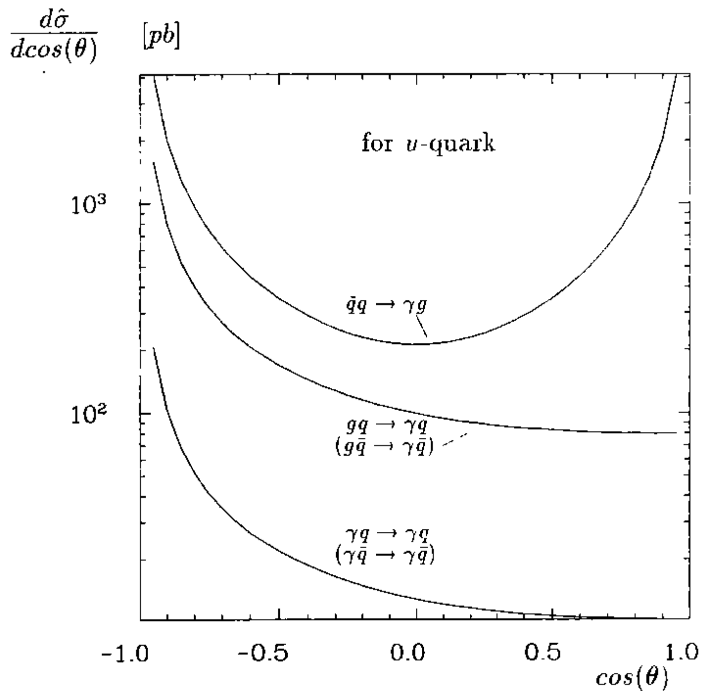

Figure 19: The partonic cross section for subprocesses $ab \to cd$ involving one photon in the final state as a function of the scattering angle $cos(\theta)$ between partons a and c in the ab centre-of-mass for the invariant mass $M = \sqrt{s} = 50$ GeV.

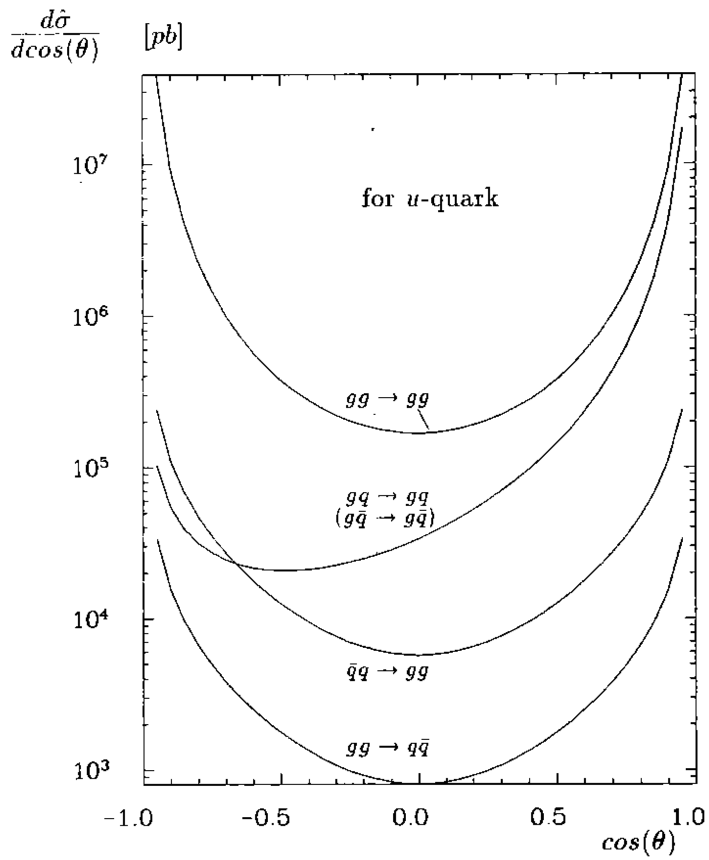

Figure 20: The partonic cross section for subprocesses $ab \to cd$ involving gluons and quarks in the final state as a function of the scattering angle $cos(\theta)$ between partons a and c in the ab centre-of-mass for the invariant mass $M = \sqrt{s} = 50$ GeV.

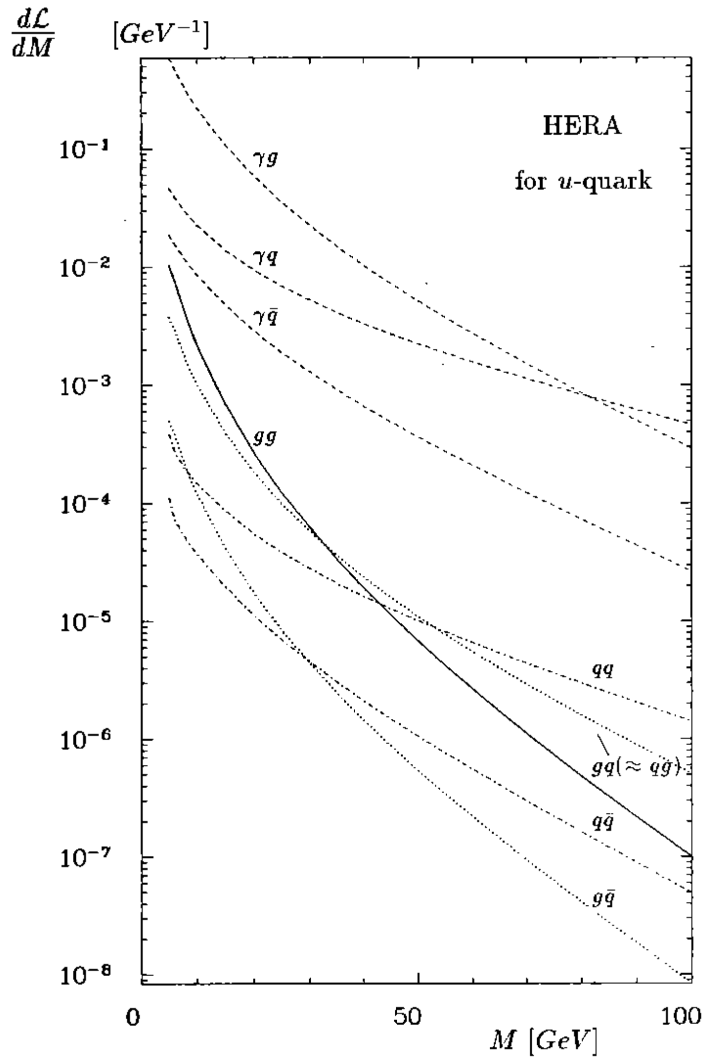

Figure 21: The parton luminosity for subprocesses involving photons (dashed lines), gluons with quarks/antiquarks (dotted lines), gluon-gluon (full line) and quarks only (dashed-dotted lines) for $\sqrt{S}$=314 GeV. M is the invariant mass of the listed partons. Note that the label $q(\bar{q})$ denotes the $u(\bar{u})$-quark. The first label refers to the photon component whereas the second one refers to the parton originating from the proton.

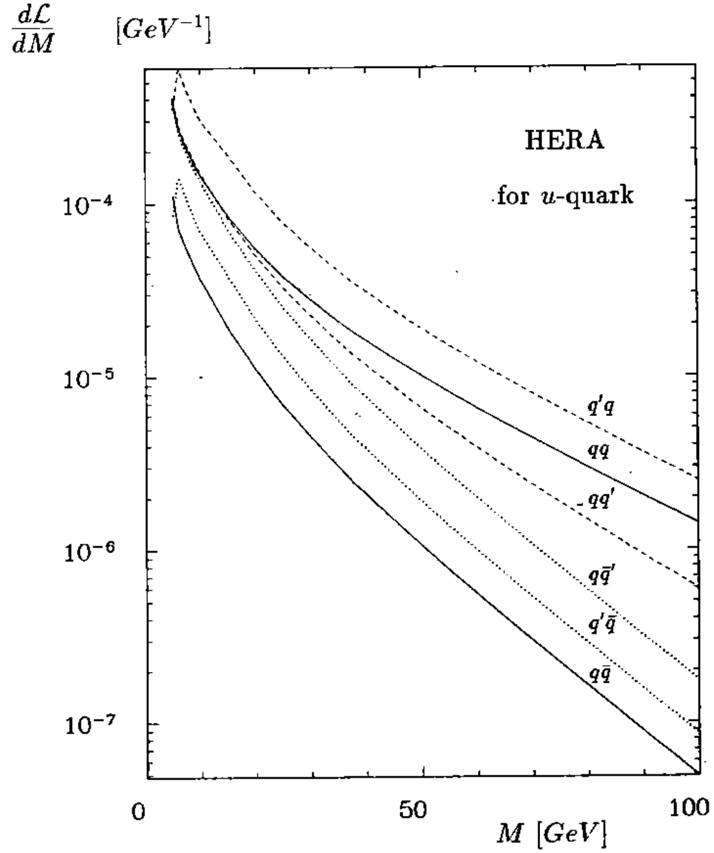

Figure 22: The parton luminosity for subprocesses involving quarks only for $\sqrt{S}$=314 GeV. M is the invariant mass of the listed partons. Note that the label $q(\bar{q})$ denotes the $u(\bar{u})$-quark while q' and $\bar{q}'$ refer to a sum over the d, s, c, b-quarks and antiquarks respectively. The first label refers to the photon component whereas the second one refers to the parton originating from the proton.

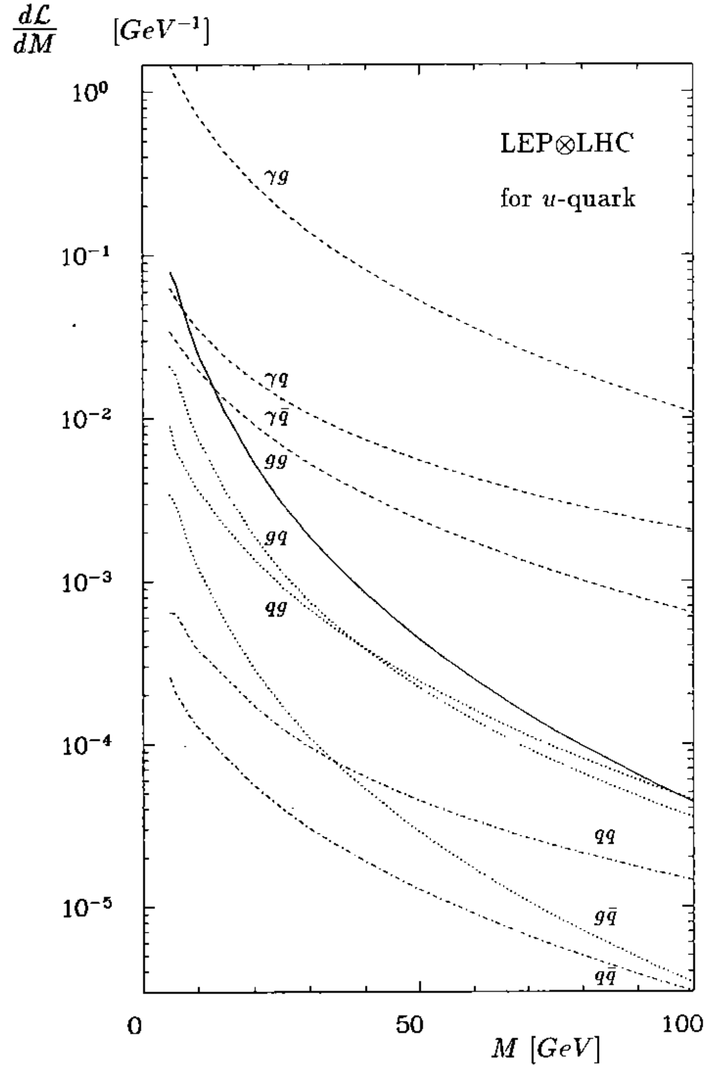

Figure 23: The parton luminosity for subprocesses involving photons (dashed lines), gluons with quarks/antiquarks (dotted lines), gluon-gluon (full line) and quarks only (dashed-dotted lines) for $\sqrt{S}$=1.3 TeV. M is the invariant mass of the listed partons. Note that the label $q(\bar{q})$ denotes the $u(\bar{u})$-quark. The first label refers to the photon component whereas the second one refers to the parton originating from the proton.

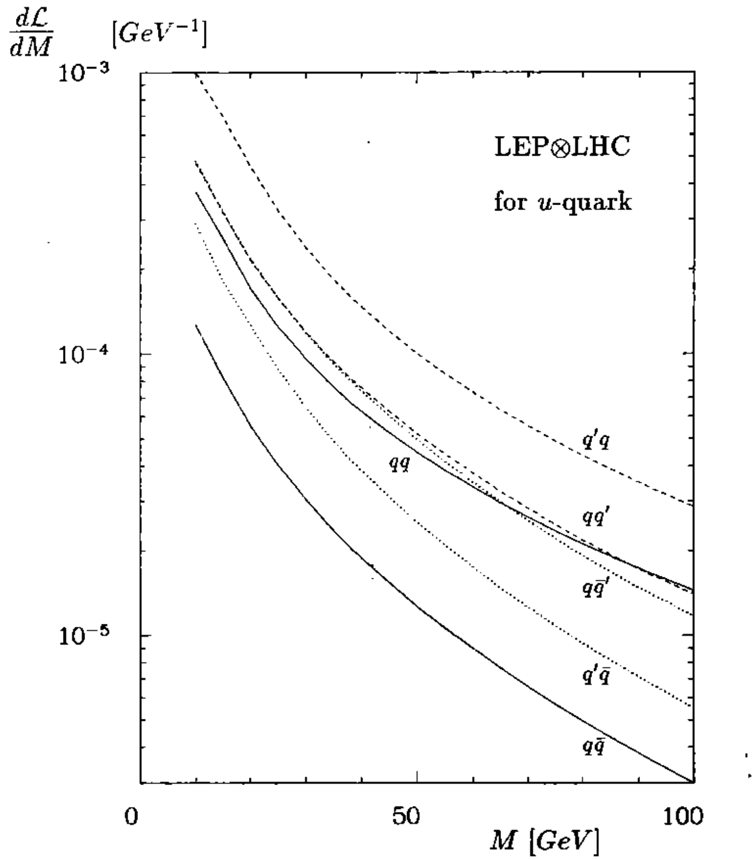

Figure 24: The parton luminosity for subprocesses involving quarks only for $\sqrt{S}$=1.3 TeV. M is the invariant mass of the listed partons. Note that the label $q(\bar{q})$ denotes the $u(\bar{u})$-quark while q' and $\bar{q}'$ refer to a sum over the d, s, c, b-quarks and antiquarks respectively. The first label refers to the photon component whereas the second one refers to the parton originating from the proton.

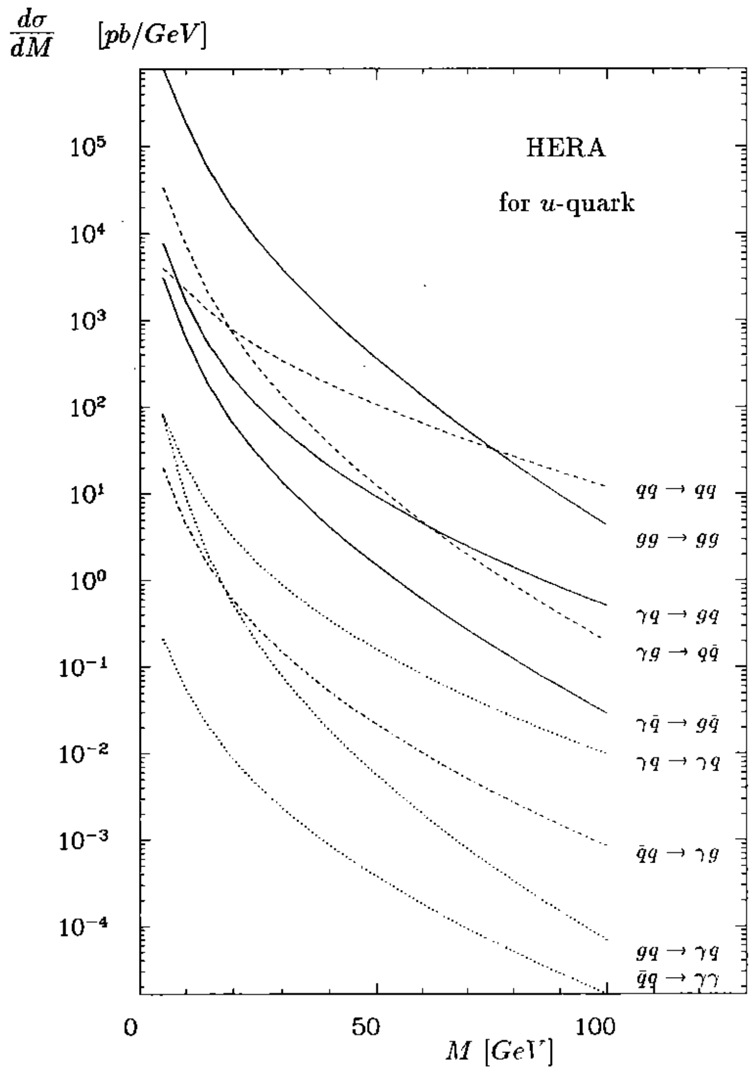

Figure 25: The ep cross section for subprocesses involving photons (dotted lines), gluons (full lines) and quarks only (dashed lines) in the final state for $\sqrt{S}$=314 GeV. M is the invariant mass of the outgoing partons. Note that $q(\bar{q})$ denotes the $u(\bar{u})$-quark. The first label refers to the photon component whereas the second one refers to the parton originating from the proton.

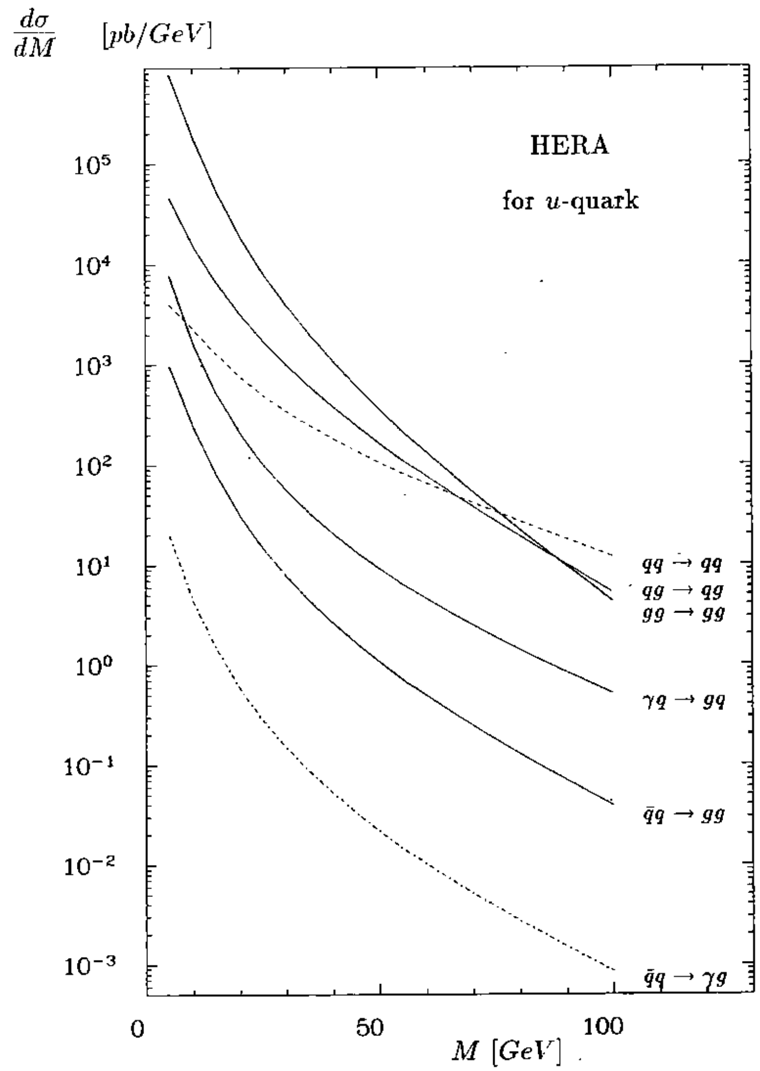

Figure 26: The ep cross section for subprocesses involving gluons in the final state and $qq \to qq$ (see text) for $\sqrt{S}$=314 GeV. M is the invariant mass of the outgoing partons. Note that the label $q(\bar{q})$ denotes the $u(\bar{u})$-quark. The first label refers to the photon component whereas the second one refers to the parton originating from the proton.

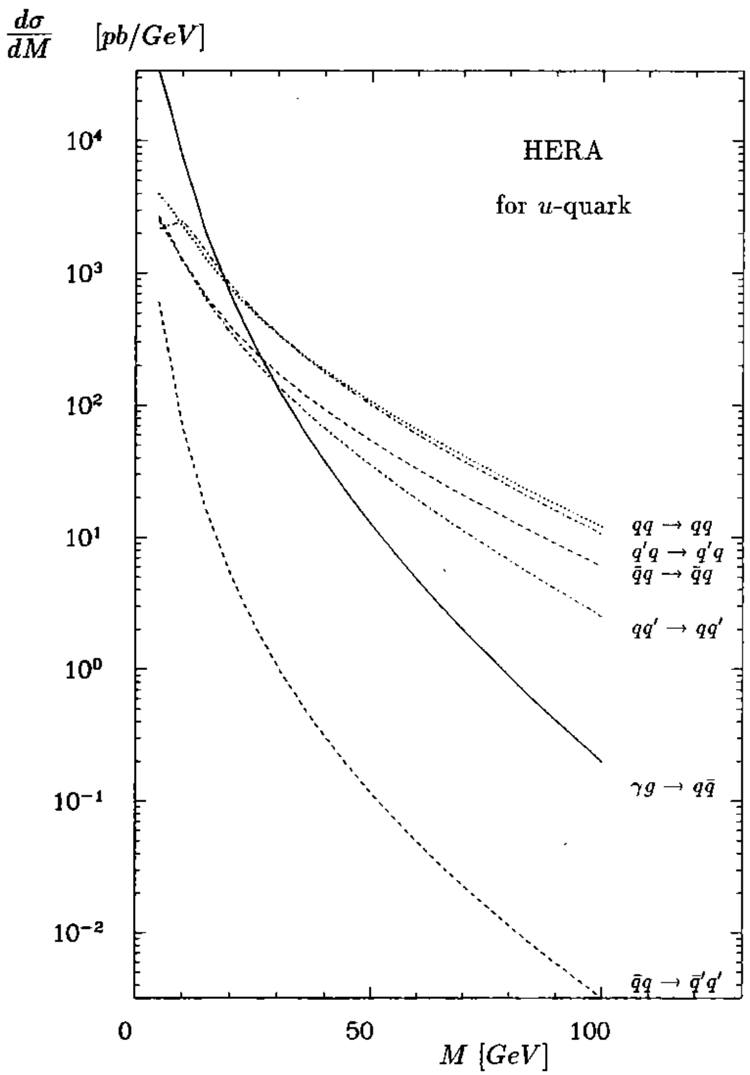

Figure 27: The ep cross section for subprocesses involving quarks in the final state for $\sqrt{S}$=314 GeV. M is the invariant mass of the outgoing partons. Note that the label $q(\bar{q})$ denotes the $u(\bar{u})$-quark while q' and $\bar{q}'$ refer to a sum over the d, s, c, b-quarks and antiquarks respectively. The first label refers to the photon component whereas the second one refers to the parton originating from the proton.

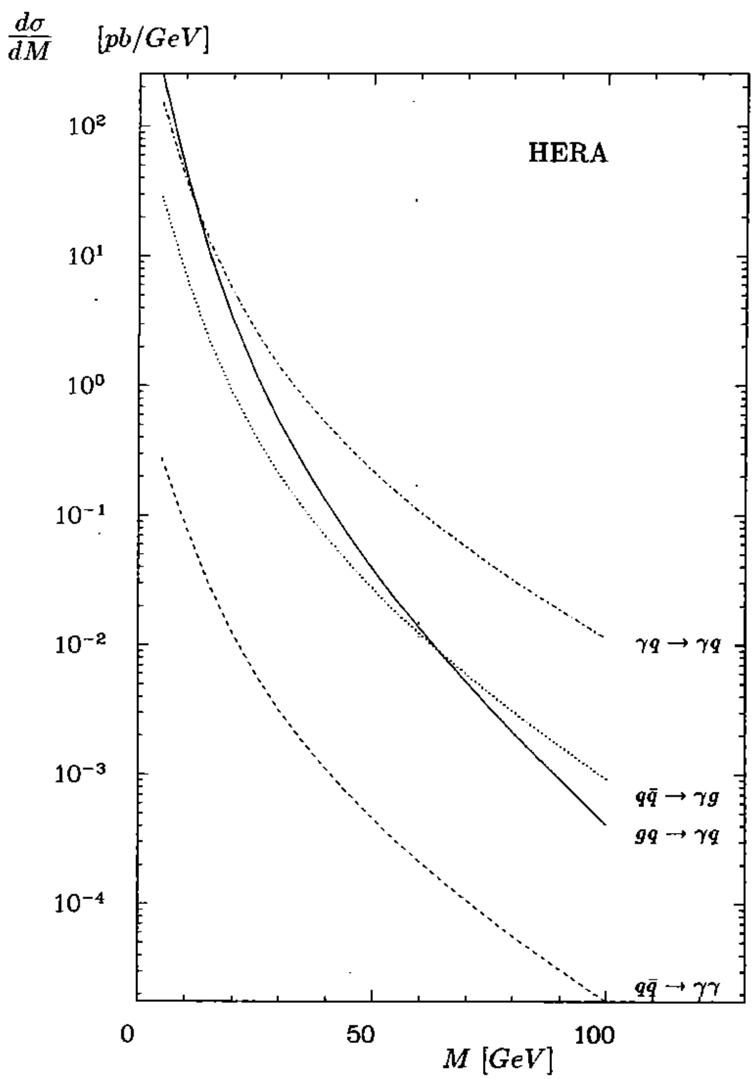

Figure 28: The ep cross section for subprocesses leading to photons in the final state for $\sqrt{S}$=314 GeV. M is the invariant mass of the outgoing partons. Note that here q refers to a sum over the d, u, s, c, b-quarks and their anti-quarks in the proton; the label $q\bar{q}$ denotes a sum over all pairs $q\bar{q}$ in the photon and the proton; the label gq refers to a sum over all pairs of quarks(antiquarks) and gluons in the photon and the proton.

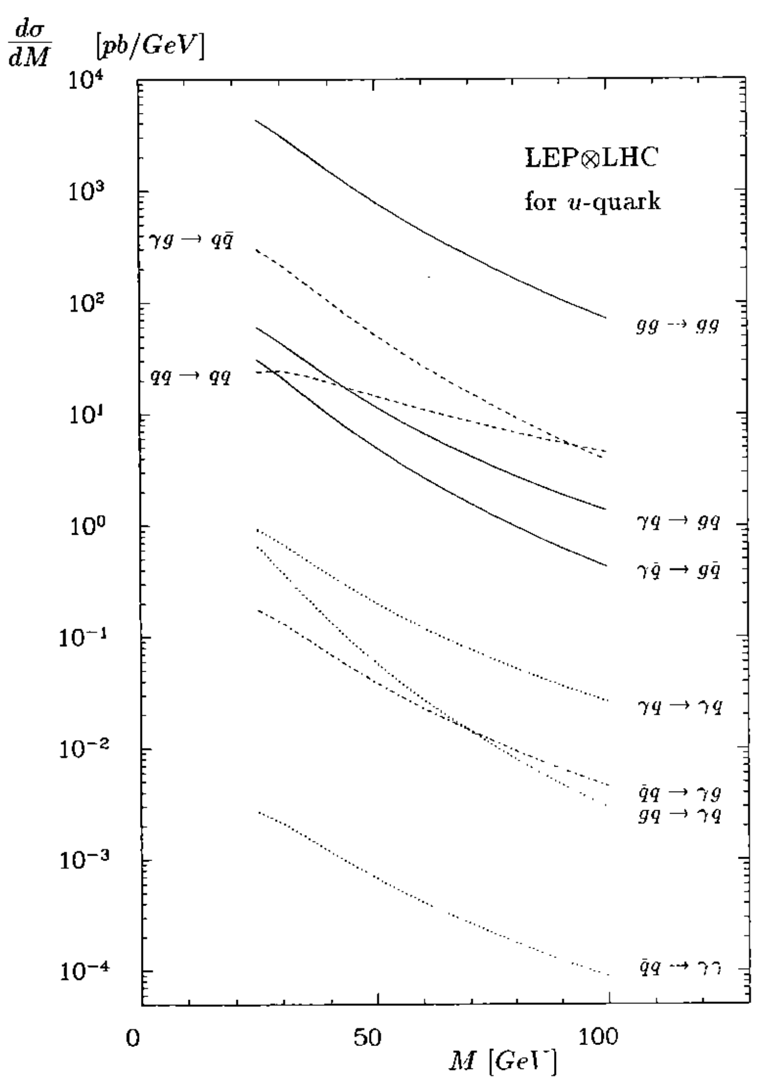

Figure 29: The ep cross section for subprocesses involving photons (dotted lines), gluons (full lines) and quarks only (dashed lines) in the final state for $\sqrt{S}$=1.3 TeV. M is the invariant mass of the outgoing partons. Note that $q(\bar{q})$ denotes the $u(\bar{u})$-quark respectively. The first label refers to the photon component whereas the second one refers to the parton originating from the proton.

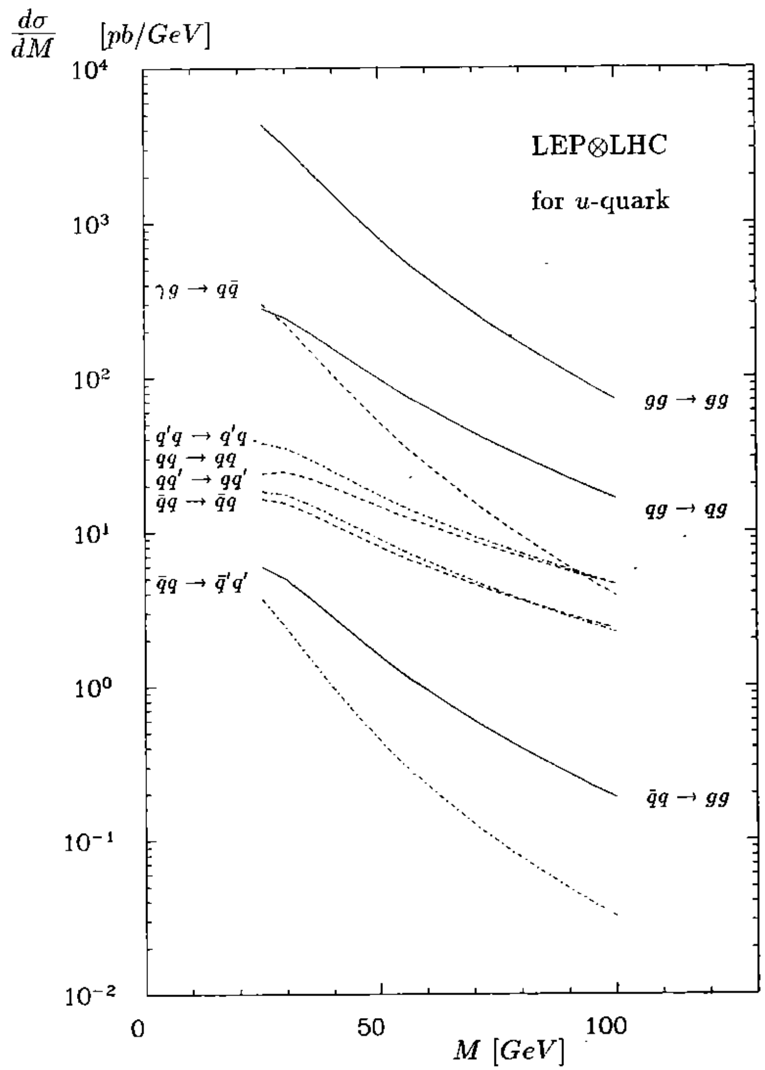

Figure 30: The ep cross section for subprocesses involving gluons in the final state (full lines) and quarks only (dashed and dashed-dotted lines) for $\sqrt{S}$=1.3 TeV. M is the invariant mass of the outgoing partons. Note that the label $q(\bar{q})$ denotes the $u(\bar{u})$-quark while q' and $\bar{q}'$ refer to a sum over the d, s, c, b-quarks and antiquarks respectively. The first label refers to the photon component whereas the second one refers to the parton originating from the proton.

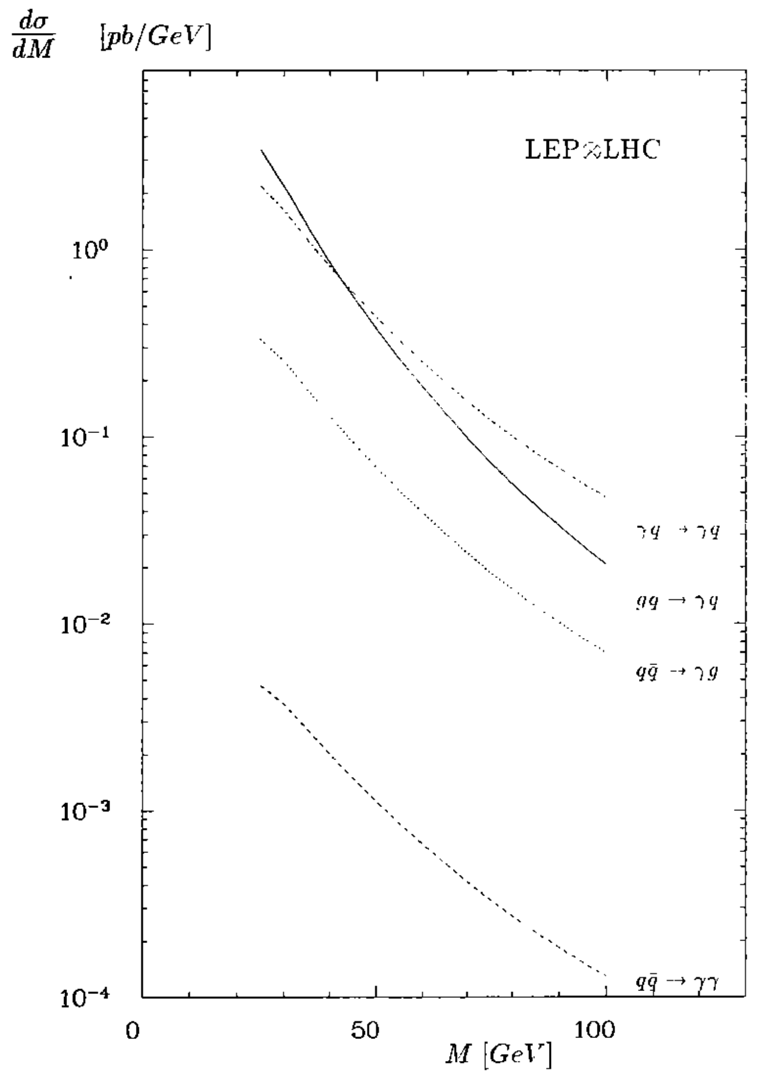

Figure 31: The ep cross section for subprocesses leading to photons in the final state for $\sqrt{S}$=1.3 TeV. M is the invariant mass of the outgoing partons. Note that here q refers to a sum over the d, u, s, c, b-quarks and their anti-quarks in the proton; the label $q\bar{q}$ denotes a sum over all pairs qq in the photon and the proton; the label gq refers to a sum over all pairs of quarks(antiquarks) and gluons in the photon and the proton.